



**HAL**  
open science

# Reaching the human scale: A spatial and temporal downscaling approach to the archaeological implications of paleoclimate data

Daniel Contreras, Joel Guiot, Romain Suarez, Alan Kirman

## ► To cite this version:

Daniel Contreras, Joel Guiot, Romain Suarez, Alan Kirman. Reaching the human scale: A spatial and temporal downscaling approach to the archaeological implications of paleoclimate data. *Journal of Archaeological Science*, 2018, 93, pp.54-67. 10.1016/j.jas.2018.02.013 . hal-01789786

**HAL Id: hal-01789786**

**<https://hal.science/hal-01789786>**

Submitted on 16 May 2018

**HAL** is a multi-disciplinary open access archive for the deposit and dissemination of scientific research documents, whether they are published or not. The documents may come from teaching and research institutions in France or abroad, or from public or private research centers.

L'archive ouverte pluridisciplinaire **HAL**, est destinée au dépôt et à la diffusion de documents scientifiques de niveau recherche, publiés ou non, émanant des établissements d'enseignement et de recherche français ou étrangers, des laboratoires publics ou privés.

1 REACHING THE HUMAN SCALE:  
2 A SPATIAL AND TEMPORAL DOWNSCALING APPROACH TO THE ARCHAEOLOGICAL  
3 IMPLICATIONS OF PALEOCLIMATE DATA  
4

5 Daniel Contreras<sup>1,2</sup>, Joel Guiot<sup>3</sup>, Romain Suarez<sup>4</sup>, and Alan Kirman<sup>5</sup>  
6

- 7 (1) Institut Méditerranéen de Biodiversité et d'Ecologie marine et continentale (IMBE),  
8 Aix Marseille Université, CNRS, IRD, Avignon Université, Aix-en-Provence, France  
9 ([danielalexandercontreras@gmail.com](mailto:danielalexandercontreras@gmail.com))  
10 (2) Groupement de recherche en économie quantitative d'Aix-Marseille (GREQAM),  
11 Aix-Marseille Université, France  
12 (3) Aix-Marseille Université, CNRS, IRD, Coll France, CEREGE, Aix-en-Provence,  
13 France  
14 (4) Aix-Marseille Université, LabEx OT-Med, Aix-en-Provence, France  
15 (5) CAMS-EHESS, Ecole des Hautes Etudes en Sciences Sociales and Aix-Marseille  
16 Université  
17

18 **Abstract**

19 Assessing the implications of paleoclimatic and paleoenvironmental data at temporal  
20 and spatial scales that would have directly intersected with human decision-making and  
21 activity is a fundamental archaeological challenge. This paper addresses this challenge by  
22 presenting a spatial and temporal downscaling method that can provide quantitative high-  
23 spatio-temporal-resolution estimates of the local consequences of climatic change. Using a  
24 case study in Provence (France) we demonstrate that a centennial-scale Mediterranean-wide  
25 model of Holocene climate, in conjunction with modern geospatial and climate data, can be  
26 used to generate explicit and solidly-grounded monthly estimates of temperature,  
27 precipitation, and cloudiness at landscape scales and with annual resolution, enabling  
28 consideration of climate variability at human scales and meeting the data requirements of  
29 socioecological models focused on human activity. While the results are not reconstructions  
30 – that is, particular values are single realizations, consistent with the coarse-grained data but  
31 not individually empirically derived nor unique solutions – they provide a more suitable basis  
32 for assessing the human consequences of climate change than can coarse-grained data.  
33

34 **Keywords:** downscaling; resolution; scale; paleoclimate; climate change; human-  
35 environment interactions  
36

37 **1. Introduction**  
38

39 Interpreting the consequences of environmental change for past peoples is a  
40 longstanding concern of archaeology, and often the ‘hook’ for paleoclimatic or  
41 paleoenvironmental studies as well. Developing explanatory links has remained a persistent  
42 challenge, however, and studies that are able to move beyond correlation to causation remain  
43 rare. Much of this difficulty results from the challenge of assessing the implications of  
44 paleoclimatic and paleoenvironmental data at temporal and spatial scales that would have  
45 been directly relevant to human decision-making and activity. We address this problem by  
46 developing a spatial and temporal downscaling method that can provide quantitative high-  
47 spatiotemporal-resolution estimates of the local consequences of climatic change. Using a  
48 case study in Provence we demonstrate that a centennial-scale Mediterranean-wide model of  
49 Holocene climate, in conjunction with modern geographic and climatic data, can be used to  
50 generate solidly-grounded monthly estimates of temperature, precipitation, and cloudiness at a

51 300m spatial scale and with annual resolution. These results, it must be emphasized, are not  
52 reconstructions: they are single realizations consistent with coarse-grained data, but individual  
53 values are not directly empirically derived. Downscaling generates one set of values  
54 consistent with the coarse-grained input data, but the results are not unique solutions  
55 (Bierkens et al., 2000, p. 111; Wu and Li, 2006, p. 35). However, they provide a more  
56 suitable basis for assessing the human consequences of climate change than can coarse-  
57 grained data, as analyses of past human-environment interaction grounded in anthropological  
58 archaeology require high spatial and temporal resolution. Anthropological archaeological  
59 explanation relies on theoretical models of human behavior and decision-making that are  
60 necessarily grounded in human experience: spatial and temporal scales measured in hectares  
61 and years rather than regions and centuries.

62 In this paper we review these issues of scale and resolution in the study of past human-  
63 environment interactions before demonstrating how spatial and temporal downscaling has the  
64 potential to address the challenge of relating spatially and temporally coarse-grained  
65 paleoclimate data to fine-grained anthropologically-grounded explanations of past human  
66 behavior. We explore the application of spatial downscaling of paleoclimate data to provide  
67 high spatial resolution, and temporal downscaling to provide high temporal resolution. This  
68 combined approach enables consideration of landscape-scale spatial variability in past  
69 climates (vital in topographically diverse landscapes in which climate effects would not have  
70 been spatially uniform) as well as consideration of interannual variability. Such downscaling  
71 is a necessary tool for considering the human consequences of climate changes documented in  
72 spatial and temporal aggregate.

## 74 **2. Scale and Resolution in the study of past human-environment interactions**

76 Description and analysis of past human-environment interactions, particularly over the  
77 long-term, comprises a fundamental goal of archaeology. This focus underlies several of the  
78 recently-articulated “grand challenges for archaeology” (Kintigh et al., 2014), and has been  
79 singled out in 21<sup>st</sup> century discussions of the discipline as central to archaeology’s  
80 contribution to interdisciplinary efforts to understand past and present socioenvironmental  
81 systems, as well as of pressing modern relevance (e.g., Van der Leeuw and Redman, 2002;  
82 Smith et al., 2012).

83 Analysis of long-term human-environment interactions promises improved  
84 understanding of both cultural and environmental trajectories, and provides a tool for  
85 examining the anthropogenic component of past and modern environment and climate. It is  
86 fundamental to ongoing debates over the Anthropocene, in which archaeologists,  
87 paleoenvironmental scientists, and geologists dispute the antiquity, character, and significance  
88 of that period (e.g., Braje, 2015; Crutzen and Steffen, 2003; Erlandson and Braje, 2013;  
89 Morrison, 2015; Ruddiman, 2013; Smith and Zeder, 2013; Zalasiewicz et al., 2015).

90 However, such analysis continues to be challenged by problems of spatial and  
91 temporal scale and resolution (cf. Contreras, 2017). The problem is not unique to  
92 archaeology, but central also to modern discussions of climate change: what are the local  
93 consequences of global climate? In analytical terms, how can we move from global summary  
94 data to local characterizations that enable consideration of the human consequences of climate  
95 change? Moreover, as the global effects of local behaviors can also be significant for large-  
96 scale modeling, the inverse problem is also an important focus: in order to estimate the  
97 aggregate global impact of local behaviors, those behaviors must themselves be modeled,  
98 taking into account how diverse actors respond to local conditions.

99 The need to reconcile contrasting scales and resolutions results partly from evidentiary  
100 constraints, and partly from contrasting foci and explanatory mechanisms of archaeology on

101 the one hand and paleoclimatic and paleoenvironmental science on the other. Paleoclimatic  
102 and paleoenvironmental science often strives to achieve regional and long-term relevance,  
103 resulting in coarser (regional and centennial) scales of analysis. In contrast, archaeological  
104 explanation relies fundamentally on anthropological models of behavior – i.e., understandings  
105 of human activity that are grounded in decision-making at local and annual scales. As a  
106 result, linking analyses that focus on distinct scales, with varying resolutions, is vital to  
107 relating archaeological and paleoclimatic and paleoenvironmental data, and has been the  
108 focus of both practical and theoretical consideration in archaeology (e.g., Stein, 1993; Lock  
109 and Molyneaux, 2006; Robb and Pauketat, 2013; Kintigh and Ingram, 2018). Nevertheless,  
110 analysis (and even description) of human-environment interaction remains difficult at best  
111 with coarse-grained data, and must confront basic questions of scale and resolution: In space,  
112 what do regional-scale data mean for landscape-scale experience, and in time, what do  
113 centennial-scale data mean for annual or seasonal experience?

114 This problem is endemic to applications of regional modeling to archaeological  
115 explanation (cf. Brayshaw et al., 2011, p. 28): even when they succeed in revealing interesting  
116 patterning, coarse-grained models can suggest broad correlations but require finer-grained  
117 analyses if explanatory linking mechanisms are to be pursued. High-resolution empirical data  
118 might be ideal, but it is (given the character of paleoclimatic, paleoenvironmental, and  
119 archaeological archives) rare and spatially and temporally uneven. In their absence, when  
120 only a limited number of observations for a broad area with varied topography may be  
121 available from recorded and/or modeled data, it is possible to take modern data from that area  
122 and, presuming the climate-geography relationships to have remained relatively constant over  
123 time, reconstruct realistically spatially variable climate data. Similarly, modern (recorded)  
124 interannual variability can serve as the basis for realistically modeling temporal variability in  
125 climate variables. Spatial and temporal downscaling thus offer a way of taking advantage of  
126 uneven data to explore potential linking mechanisms between climate variables and human  
127 behavior, and ultimately to develop arguments that move from correlation to explanation.

128

## 129 2.1 Downscaling

130

131 Downscaling addresses the problem of deriving small-scale values from large-scale  
132 aggregates (Bierkens et al., 2000, pp. 111–118; Wilby et al., 2004; Wu and Li, 2006, pp. 34–  
133 36). The principle is that any summary value is by its definition a product of a number of  
134 possible individual values that even when not precisely known can be probabilistically  
135 estimated. We focus here on statistical downscaling of low-resolution climatic data to enable  
136 generation of climate variables at the landscape scale. This is based on applying relationships  
137 between high-resolution and low-resolution fields, calibrated based on time periods where  
138 both exist, to the target low-resolution field.

139 The climate-modeling community has explored downscaling of climate data,  
140 stimulated by the desire to address regional impacts of climate change in scenarios where  
141 global climate models (GCMs) are the primary data source (cf. Fowler et al., 2007; Wilby et  
142 al., 2004). The focus has primarily been on future impacts, but the paleoclimate community  
143 (e.g., Korhonen et al., 2014; Levavasseur et al., 2011; Vrac et al., 2007) has also begun to  
144 explore the potential of downscaling methods as means of examining regional or implications  
145 of global models of past climate. Geographically-based downscaling (e.g., Joly et al., 2010;  
146 Martin et al., 2013; Vrac et al., 2007) is one means of dealing with spatially heterogeneous  
147 landscapes, and is particularly valuable for applications to past climates, as geographic  
148 variables are generally stable over archaeological timescales, whereas regional climate  
149 relationships to GCMs may have been significantly different in the past (cf. Vrac et al., 2007,  
150 p. 670).

151 Geographically-based methods which have been applied to paleoclimatological data  
152 are based on the calibration of potentially non-linear relationships between the target high-  
153 resolution variable and its low-resolution version completed by high-resolution geographical  
154 variables (topography, distance to sea, etc.; see Vrac et al., 2007). The most appropriate  
155 calibration technique is generally recognized to be a generalized additive model (GAM)  
156 (Hastie and Tibshirani, 1990) or a multinomial logistic GAM when the variable to  
157 interpolate is categorical (Levavasseur et al., 2011, 2013), but other geostatistical methods  
158 have also been explored (e.g., Joly et al., 2010; Martin et al., 2013). With fewer potential  
159 predictors available at higher spatial resolution and for the past, we have used simple  
160 regression to select predictor variables (described in Section 3.2.1, below).

161

## 162 2.2 Downscaling for Archaeology – Potentials and Limitations

163

164 Archaeologists, given their field's long interest in human-environment interactions,  
165 are often avid consumers of paleoclimate data. However, the potential of downscaling has  
166 been largely neglected (with important recent exceptions; see Burke et al., 2014; Gauthier,  
167 2016). When downscaling has been explored the target scales have, following the climate  
168 work, been regional (with the notable recent exception of Bocinsky and Kohler, 2014).

169 Spatial and temporal downscaling produces values for climate variables that, for any  
170 given pixel in any given year, are in all probability inaccurate: they are single realizations and  
171 not unique solutions. However, in aggregate the fidelity to the areal and temporal means  
172 represented by the input paleoclimate data is high, and is based on the reasonable assumptions  
173 that 1) modern relationships between climate and geographic variables applied also in the  
174 past, and 2) 20<sup>th</sup> century interannual variability resembles past interannual variability. While  
175 the second assumption in particular may be questionable, in the absence of a local annually-  
176 resolved paleoclimate archive a better model for interannual variability is unavailable.

177 As in any modeling exercise, the data employed might also be critiqued. The spatial  
178 and temporal downscaling approach presented here can be applied to virtually any input data,  
179 but the accuracy of the results is wholly dependent on the accuracy of those data.  
180 Comparisons across space and time within the same dataset, however, can minimize the  
181 problem of absolute accuracy of results, and in principle one might also vary the input data if  
182 multiple sources were available.

183 As archaeologists are commonly consumers of paleoclimate data, the archaeological  
184 use of climate data – whether from GCMs or derived (as in our case study below) from  
185 paleoclimatic reconstructions – is likely to be offline (using previously generated results)  
186 rather than coupled to runs of global and/or regional models. Inasmuch as that is the case,  
187 archaeologists are more likely to employ statistical downscaling than dynamical downscaling  
188 (cf. Fowler et al., 2007, pp. 1548–1552). Although the latter – coupled models able to both  
189 incorporate and enable investigation of feedbacks between human activity and climate  
190 dynamics – perhaps have the most analytical promise (cf. Wilby et al., 2004, p. 11 on human-  
191 climate feedbacks for contemporary and future models and Kaplan et al., 2010 on the  
192 significance of past human activity for regional and global climate), they are also the most  
193 complex conceptually and computationally. We address here the less optimal but  
194 nevertheless vital statistical downscaling of pre-existing climate data, which represents the  
195 more likely scenario for most archaeological practitioners and still promises to enhance  
196 archaeological interpretation of the local consequences of past climates.

197 Even offline, working with extant paleoclimate data/reconstructions, spatial and  
198 temporal downscaling has significant potential to enable analytical consideration of human-  
199 environment interactions at the scale and resolution necessary to consider the human  
200 consequences of climate change. Box's dictum that "all models are wrong" (Box, 1979) is

201 apropos, and we argue that a downscaling approach produces data that are more useful in  
202 archaeological interpretation, and less misleading, than implicit models that posit uniform  
203 climate over a large area and over long timespans. It is important to emphasize that using  
204 paleoclimate data in archaeological interpretations *without* downscaling is *also* an exercise in  
205 modeling: it posits a direct one-to-one relationship between local and annual climates and  
206 spatially and temporally averaged regional climate data. That being the case, we suggest that  
207 consideration of the implications virtually any method of downscaling is likely to improve  
208 archaeological interpretation.

209 The human experience of climate is fundamentally local and annual (if not in fact  
210 seasonal), and the consequences of changes in climate are quotidian even if they are measured  
211 in aggregate. While the use of global or regional paleoclimate data that is rarely sub-decadal  
212 (and often much coarser) reflects the reality of data availability for most archaeological  
213 research, a downscaling approach makes it possible to explicitly consider the local and annual  
214 implications of such data. This can also provide the requisite spatially explicit and  
215 quantitative basis for further modeling that addresses particular questions about the human  
216 past, especially past human-environment interactions, including agricultural niche modeling  
217 (e.g., Bocinsky and Kohler, 2014; d'Alpoim Guedes et al., 2016), agroecosystem modeling  
218 (e.g., Contreras et al., in press), agent-based modeling of subsistence activity (e.g., Barton et  
219 al., 2010; Kohler et al., 2012), and isoscape modeling (e.g., Kootker et al., 2016; Willmes et  
220 al., 2018). The higher resolution produced by downscaling can enable models suited to  
221 construction of more robust arguments about the implications of past environmental change  
222 for human experience.

223 Preindustrial agriculture is a likely mechanism linking changing climates to  
224 socioeconomic change (Currie et al., 2015; Schwindt et al., 2016), making the relationship of  
225 settlement distributions to climate variables a potential means of examining human  
226 ecodynamics. Archaeologists have attempted to reconstruct past ecodynamics by, for  
227 example, comparing archaeological settlement patterns against spatial patterning of modern  
228 maize productivity in Central Mexico (Gorenflo and Gale, 1986) or against potato and maize  
229 productivity in the Central Andes (Seltzer and Hastorf, 1990). More recent efforts have  
230 involved sophisticated digital modeling of precipitation-limited maize agriculture in the U.S.  
231 Southwest (Bocinsky and Kohler, 2014) or temperature-limited cereal agriculture on the  
232 Tibetan Plateau (d'Alpoim Guedes et al., 2016). Questions of scale and resolution are critical  
233 to the employment of these models, as topographic and climatic diversity can combine to  
234 create viable niches within larger areas that are apparently unsuitable. As the example of the  
235 Central Andes demonstrates, the potential exploitation (as well as creation and management,  
236 cf. (Erickson, 2000; Mamani Pati et al., 2011)) of microclimates as agricultural niches  
237 suggests the importance of fine-grained analysis and consideration of the potential plasticity  
238 of thresholds.

239 A fourth dimension of variability can also be critical: both interannual variability and  
240 change over time can be vital parameters for inhabitants. Temporal downscaling enables  
241 some consideration of interannual variability, potentially vital in areas where long-term means  
242 are poor summaries of annual experience (e.g., where interannual variability is high). In areas  
243 where agricultural or foraged resources are near biological thermal or hydrologic limits (or  
244 even economic ones), long-term means may be poor indicators of subsistence viability, as  
245 periodic low minima may be an unacceptable risk. Re-aggregation of climate data over  
246 various timespans can also enable direct comparison of one archaeological period to another,  
247 for instance across archaeologically significant thresholds.

248  
249

250 **3. Applying Downscaling in Archaeology: A Case Study in Holocene Provence (France)**

251 We illustrate the data requirements, spatial and temporal downscaling methods, and  
252 interpretive payoffs with an example from Holocene Provence.

### 253 3.1 Data

254 We present here a computational approach that uses modern (20<sup>th</sup>-21<sup>st</sup> century)  
255 CNRM2014<sup>1</sup> and CRU TS v. 3.23<sup>2</sup> climate data to relate climatic variables (temperature,  
256 precipitation, and cloudiness) to geographic variables (primarily elevation and distance-from-  
257 the-sea<sup>3</sup>) through geographically-weighted regression. As the geographic variables are of  
258 high spatial resolution where the climate variables are coarse (even for modern data), this  
259 relationship can then be used to predict values of climate variables at high spatial resolution.

260 The problem of temporal resolution is in turn addressed by generating interannual  
261 variability within reconstructed trends based on the estimated past seasonal amplitudes and  
262 the interannual variability of the modern data. For case study region in Provence that we use  
263 here (a topographically diverse 40 km x 40 km area; see Figure 1), Guiot and Kaniewski's  
264 (2015) Holocene climate reconstruction (HolCR) based on inverse vegetation modeling with  
265 data from 295 pollen cores provides monthly reconstructions of average daily temperature  
266 (ADT), total monthly precipitation (TMP), and % cloudiness (CLD) (see Figure 2). These  
267 monthly values for temperature, precipitation, and % cloudiness are provided at centennial  
268 steps throughout the Holocene<sup>4</sup>, but the 2° (latitude) by 4° (longitude) spatial resolution  
269 (approximately 225 x 450 km cells at Mediterranean latitudes) means that for the study area  
270 we use here only a single value for each variable is available. Modern data are higher  
271 resolution: for average daily temperature (TAV) and average daily precipitation (PAV) data  
272 are available on an 8km grid from the CNRM2014 simulation for the period 1951-2005, while  
273 cloudiness (CLD) data is available for the period 1951-2010 at 10' resolution (approximately  
274 18 km at the latitude of the study area) from the CRU model. Calculating mean TAV and  
275 cumulative PAV for each month is necessary to relate the CRNM2014 and HolCR data.

276 The data sources and their spatial and temporal resolutions are summarized in Table 2.  
277

### 278 3.2 Methodology: A spatial and temporal downscaling approach

279 We downscale in two dimensions, addressing both spatial and temporal scales.  
280 Following the hierarchical typology established by Bierkens and colleagues (2000, pp. 111–  
281 144), these comprise distinct problems.

282 For spatial downscaling, the modern geographic and climate data described above are  
283 used to calculate relationships of geographic variables to climate variables at data points  
284 known from modern data through geographically weighted linear regression using the *spgwr*  
285 package (Bivand and Yu, 2015) in R (R Core Team, 2016). All raster processing is also  
286 carried out in R, using the *raster* package (Hijmans and van Etten, 2016) in R.

---

<sup>1</sup>A simulation model based on instrumental data, described at  
<http://www.cnrm.meteo.fr/spip.php?article125> and available from the DRIAS Portal:  
<http://www.drias-climat.fr/>

<sup>2</sup>Global coverage climate data at 0.5° resolution from 1901-2014, described in (Harris et al., 2014;  
New et al., 2002), and available at <https://5>  
[data.uea.ac.uk/cru/data/hrg/cru\\_ts\\_3.23/cruts.1506241137.v3.23/](https://5)

<sup>3</sup> Derived from the SRTM 30m digital elevation model (DEM) (NASA JPL, 2013). As detailed  
below, more environmental variables could in principle be included. In fact, for the case study, for  
each month and each climatic variable multiple environmental variables were tested and those with the  
strongest predictive value used (see Table 1).

<sup>4</sup> Available in the OT-Med data catalog at [http://database.otmed.fr/geonetnetworkotmed/srv/eng/search -  
154b9bf34-57ae-45ea-b455-9f90351e538f](http://database.otmed.fr/geonetnetworkotmed/srv/eng/search-154b9bf34-57ae-45ea-b455-9f90351e538f)

287 For temporal downscaling, the mean, trend, seasonal, and interannual values from  
288 modern data for the study area are used to generate monthly values with a modified version of  
289 the *greenbrown* package (Forkel et al., 2013; Forkel and Wutzler, 2015) in R.

290 R code for the procedures detailed below, with reference to the data sources described  
291 in Section 3.1 and Table 2, is available in the supplementary online material.

### 292 3.2.1 *Spatial downscaling*

293 The spatial downscaling that we develop here empirically relates fine-scale auxiliary  
294 information to the coarse-grained data available to derive a deterministic model.

295 Geographically-weighted regression of modern climate and geographic time-series data is  
296 used to establish functions that relate auxiliary information (geographic characteristics) to  
297 coarse-grained paleoclimate data (temperature, precipitation, and cloudiness). As even for  
298 past time periods geographic data are available at high resolution, they can be used to derive  
299 high-resolution climate variables from the existing low-resolution paleoclimate data.

300 The spatial downscaling procedure, with the input of spatially homogenous data,  
301 produces a set of spatial relationships between location and climate variables that can be used  
302 to calculate spatially variable rasters of climate variables at temporal resolution that matches  
303 the input data. In our case study, this makes possible high-spatial-resolution climate data at  
304 centennial steps throughout the Holocene (following the resolution of Guiot and Kaniewski's  
305 dataset).

306 Using a DEM larger than the study area ( $\sim 3100 \text{ km}^2$  rather than  $\sim 1400 \text{ km}^2$ ), in order  
307 to increase the sample of CNRM2014 points, relationships of geographic variables to climate  
308 variables at each point are calculated by geographically weighted linear regression. After  
309 extracting values from the rasters of the geographic variables at each point where there are  
310 CNRM2014 values for climate variables, regressions are calculated to test the value of  
311 various geographic variables as predictors of climate variables, and then to estimate the  
312 climatic variables using the values of the selected geographic variables.

313 Geographic variables that are the strongest predictors for our case study (determined  
314 by linear regression using the entire dataset of 54 climate datapoints in the  $\sim 3100 \text{ km}^2$  area)  
315 are elevation and distance from the sea. Irradiance – calculated in GRASS GIS (GRASS  
316 Development Team, 2016) with *r.sun.daily* – and latitude were also tested; neither is a  
317 significant predictor, likely as the CNRM2014 data are too spatially sparse to correlate with  
318 highly locally-variant environmental characteristics such as irradiance, aspect, topographic  
319 roughness, etc. Modern climate data of higher spatial-resolution would allow incorporation  
320 of more predictive variables, but even with only two predictor variables that the predictive  
321 values are fairly high: mean  $R^2$  values (across all months) are .93 for temperature, .80 for  
322 precipitation, and .77 for cloudiness. These regressions, in other words, can predict climate  
323 variables at an 8km resolution with a reasonable degree of confidence, and can thus be used to  
324 predict values of climate variables on the basis of geographic variables at finer spatial  
325 resolutions – i.e., limited in spatial resolution by the latter but not the former.

326 The selected geographic variables are then used in a geographically-weighted  
327 regression to predict values of climate variables for each cell in a 300m pixel raster (spatial  
328 resolution could be increased to the limits [30m] of the original DEM with a concomitant  
329 increase in computing time<sup>5</sup>). For months and/or climate variables when linear regression  
330 indicates that distance from the sea is not a significant predictor, elevation alone is used (see  
331 Table 1).

---

<sup>5</sup> The target resolution – here 300m – depends on analytic needs and practical concerns about computing time and subsequent data management.



332 For each cell the value of the target climate variable is predicted based on the specified  
333 geographic variables, taking into account all points for which both values are available within  
334 a specified search radius. Geographically weighted regression (gwr) works to limit the  
335 smoothing of spatial variation in the data by “moving a weighted window over the data,  
336 estimating one set of coefficient values at every chosen ‘fit’ point.” (Bivand, 2015); that is,  
337 relationships between geographic and climate variables can vary locally rather than being  
338 based necessarily on a regression across the entire dataset. In the case study here the  
339 difference between gwr and other methods is not large, but with denser data or a more  
340 spatially variable dataset gwr would in principle be preferable, as it would mirror, rather than  
341 smoothing, spatial heterogeneity in the input data.

342 The resulting raster is cropped to the study area. Following this method a raster is  
343 produced for each month for each climate variable. The rasters produced by this process –  
344 300m resolution, for each month – serve as reference datasets that can be adjusted according  
345 to paleoclimate data, producing high spatial-resolution estimates of paleoclimatic conditions.

### 346 3.2.2 Temporal downscaling

347 Temporal downscaling, as we employ it here, is a distinct procedure because it must  
348 operate without fine-scale auxiliary information, using a mechanistic model and conditionally  
349 stochastic methods. These comprise harmonic models with parameters derived from modern  
350 interannual variability and the long-term trends and seasonal amplitudes in the coarse-grained  
351 data. These are used to generate time-series that constitutes single realizations of the possible  
352 solutions within the parameters for the temporal scale. The result – the generation of monthly  
353 values that are consistent with the coarse-grained averages though individual values are not  
354 directly empirically derived – requires consideration of long-term trends, seasonal amplitudes,  
355 and interannual variability.

356 Centennial means of climate variables for the study area throughout the Holocene are  
357 calculated from HolCR and modern reference values for the area calculated from CNRM2014  
358 and CRU data. Centennial trends are provided by linear interpolation from the HolCR data;  
359 any three values from HolCR thus produce a continuous 200-year series, while the varying  
360 annual means of the HolCR data capture the longer-term Holocene trends. Seasonal  
361 amplitudes are calculated from HolCR by linearly interpolating the monthly values from each  
362 centennial step and fitting two-term harmonics to each decade. Temperature, precipitation,  
363 and cloudiness are calculated independently from one another. Although in principle these  
364 variables are likely to be coupled, modeling those complex and dynamic relationships (the  
365 region is influenced by both Atlantic and Mediterranean climate systems) would itself be a  
366 considerable task (Fowler et al., 2007, p. 1563). We have not attempted to model these  
367 couplings, but the covariance of these variables with the predictors should limit their  
368 divergence except in rare (stochastic) cases.

369 These trend and seasonal components are combined with interannual variability  
370 calculated from CNRM2014 and CRU data. For CNRM2014 standard deviation and range of  
371 ADT and TMP are calculated from TAV and PAV for the area from 1951 – 2005, and for  
372 CRU standard deviation and range of cloudiness values are calculated from the data for 1961  
373 - 1990 by subtracting the CRU ‘cld’ values from 100. Interannual variability throughout the  
374 Holocene apparently did not always match modern magnitudes in the region (cf. Büntgen et  
375 al., 2011; Luterbacher et al., 2006), but in the absence of specific proxy data of resolution  
376 sufficient to reconstruct interannual variability we use modern data.

377 The mean, trend, seasonal, and interannual values for the study area are used to  
378 generate monthly values for a selected time period. The `SimTs()` function from the  
379 *greenbrown* package generates monthly values for each climate variable for each year of the  
380 specified period by building a time series from multiple time-series components: the mean of  
381 the time series, the trend slope, the standard deviation of annual means, the range of annual

382 means, the seasonal amplitude, and randomly-generated short-term intra-annual variation.  
383 The sum of these components describes a time series for the selected variable (cf. Forkel et  
384 al., 2013, pp. 2118–2122). In order to fit the seasonal patterns in climate variables in the  
385 study area, we replace the cosine harmonic that `SimTs()` uses to generate a seasonal  
386 distribution with harmonics fitted to the HolCR values for the period as described above.

387 The modified `SimTs()` results are monthly values over a 200-year segment, from  
388 which the target segment can be extracted if it is shorter. The monthly values for ADT, TMP,  
389 and % cloudiness for that segment are used to calculate monthly anomalies from the HolCR  
390 reference values, and new rasters are calculated from the reference rasters by adjusting  
391 temperature (average daily temperature in °C), precipitation (total monthly precipitation in  
392 mm), and cloudiness (% cloudcover) using the monthly anomalies for each year of the  
393 selected time window.

394 As a period of interest is defined and the data for those dates extracted from the Guiot  
395 and Kaniewski (2015) dataset, anomalies from the modern data are calculated, and the  
396 reference rasters can be used to derive rasters at 300m-resolution for any year of the Holocene  
397 for the three climate variables, all by month. To capture the trend in annual means and  
398 seasonal amplitude across a target window 200 years of data (three datapoints) are the  
399 minimum to work with. Using these in the temporal downscaling process, a time-series of  
400 spatially-downscaled rasters can be generated, from which a smaller segment can  
401 subsequently be extracted.

402

#### 403 **4. Results: From Centennial Means to a Year in Provence**

404

405 Mediterranean climate variation during the Holocene is modest compared to that of  
406 the Pleistocene, but nonetheless paleoclimate data underpins a large number of studies  
407 positing relationships between climate changes and cultural developments (see partial reviews  
408 in Finné et al., 2011; Roberts et al., 2004; Robinson et al., 2006). This is particularly true in  
409 the eastern Mediterranean (e.g., Kaniewski et al., 2015; Weninger et al., 2009; Wiener, 2014),  
410 reflecting greater abundance of archaeological and paleoclimatic research, but Holocene  
411 climate-culture links have also been suggested in the western Mediterranean (e.g., Berger and  
412 Guilaine, 2009; Carozza et al., 2015; Weinelt et al., 2015). As discussed above, the  
413 elucidation of these links is limited by chronological resolution and the often incommensurate  
414 scales of analysis and explanation pursued by paleoclimatologists and archaeologists.

415 In the Mediterranean, the diversity of microenvironments characteristic of such a  
416 topographically complex region historically has significantly complicated generalization from  
417 paleoclimate data, and further complicates the exploration of the human consequences of  
418 climate change. In Provence, geographic variability is one of the principle drivers of the  
419 region's significant environmental diversity (cf. Blondel and colleagues [2010, p. 13], who  
420 single out, "slope, exposition, distance from the sea, steepness, and parent rock type").  
421 Although of course other variables (e.g., water availability, soil depth, etc.) are also  
422 influential, environmental contrasts apparent over short distances reflect in large part the  
423 interaction of topographic variability and climatic variability. Climate changes may thus  
424 affect the spatial distribution of environmental variability as well as the environment in  
425 aggregate; both can impact the human inhabitants of a landscape. Interannual variability,  
426 which can be obscured by long-term means, may also be particularly significant for  
427 inhabitants.

428 Employing a spatial and temporal downscaling approach to explore the human  
429 consequences of past climate changes at large spatial scale and high temporal resolution to a  
430 Mediterranean case provides a means of addressing the challenges of a) reconciling scales and  
431 resolutions, and b) exploring the implications of geographic and interannual variability. The

432 case study area in Provence explores this across an approximately 1400 km<sup>2</sup> study area  
433 (Figure 1) that spans significant topographic variability: elevations range between 50 and  
434 1200 masl and the area includes both the floodplain of the Durance River and the steep  
435 limestone ridge of the Luberon. For the period for which instrumental data are available (or  
436 modeled data based directly on instrumental data; namely the CNRM2014 and CRU datasets),  
437 average daily temperatures (TAV) vary in space by 4-5 °C in each month of the year, and  
438 total monthly precipitation (TMP) by 12-32 mm (see Figure 3). Long-term temporal  
439 variation, by comparison, assessed from the HolCR dataset across the entire Holocene for the  
440 cell including the study area, is generally more modest: AMT has varied by approximately 1-  
441 2.5 °C, depending on the month, and TMP has ranged by 10-20 mm, depending on the month  
442 (see Figure 4).

443 The combination of spatial and interannual variability produces marked contrasts  
444 across the study area, belying the homogeneity fundamental to a coarse-grained  
445 reconstruction. Downscaling of AMT in the study area at 2400 BP – the coolest period of the  
446 Holocene – for instance, demonstrates both the strong seasonality recorded in the input data  
447 and the spatial variability in temperature produced by elevation gradients that is absent in the  
448 input data but produced by the downscaling process (Figure 5). AMT values from the HolCR  
449 dataset for 2400 BP range from 3.1 to 21.6 °C, while the downscaled rasters display lower  
450 minima and higher maxima, reflecting spatially variable values for each month (Table 3).

451 The addition of temporal downscaling makes it possible to move from spatially-  
452 variable but static climate reconstructions to time-series of spatially-variable reconstructions  
453 that better reflect the variable and dynamic environments that inhabitants of the region would  
454 have experienced. The addition of temporal variability following centennial trends is  
455 illustrated in Figure 6, while Figure 7 demonstrates the results of temporal downscaling to  
456 generate variability following centennial trends and modern interannual variability, in this  
457 case precipitation in the month of March for the period 4004 BP - 3096 BP, the driest period  
458 of the Holocene. Where HolCR provided a single TMP value of 36.2 mm and spatial  
459 downscaling produced a spatial range of 25.2 – 69.2 mm (Figure 7a), temporal downscaling  
460 to generate interannual variability produced a sequence of rasters whose minima range from 0  
461 – 33.9 mm and whose maxima range from 27.5 – 77.8 mm (Figure 7b; this is a single  
462 realization illustrating one possible solution).

463 These downscaled data open new analytical possibilities, particularly regarding  
464 human-environment interactions and potential impacts of climate change. Variability of the  
465 magnitude and at the spatial and temporal scales visible in Figure 7b can be vital to  
466 archaeological interpretation, and downscaling enables consideration, for instance, of whether  
467 site distributions are random with respect to climate variables. Various other factors –  
468 notably chronological resolution, landscape taphonomy, and recovery bias – make assessment  
469 of settlement pattern data in the study area an analytical challenge, but even with such  
470 challenges downscaled paleoclimate data have the potential to generate hypotheses that would  
471 have otherwise remained inaccessible.

472 The Late Iron Age expansion of settlement in the study area illustrated in Figure 8, for  
473 example, might represent a simple infilling of the landscape as population increased (push  
474 factors: local population increase, political and/or economic imperatives, etc.), and/or it might  
475 represent the results of the opening up of previously unused areas (pull factors: changes in  
476 agricultural practices or technologies [irrigation, iron plowshares, etc.]), shifts in crop  
477 preference, willingness to accept less productive land, changes in climate, etc.). Downscaled  
478 climate data make it possible to evaluate the hypothesis that changing climate enabled  
479 agricultural expansion into areas previous insufficiently productive to be exploited:  
480 comparison of the quantities and variability of precipitation in the areas settled (Figure 8)  
481 suggest little change from the Early to Late Iron Age, and the summarized values around each

482 settlement do not show any strong contrast from one period to the next (see boxplots at left in  
483 Figure 8; the climate-driven contrast in standard deviations is clearly statistically significant,  
484 but the magnitude of difference [a decline of 2% in TMP] is probably too low to suggest any  
485 notable shift in agricultural potential).

486 Higher-resolution cultural chronology, as well as specific consideration of the  
487 hydrologic needs of particular crops, might enable further evaluation of climate impacts in the  
488 3<sup>rd</sup> millennium BP. For that or any other period, resolution of the cultural chronology is a  
489 limiting factor in interpreting any effects of climate change: although the downscaled data  
490 enable tracking changing spatial patterns of climate variability, the settlement data do not  
491 always allow tracking of changes in settlement patterns at comparable temporal resolution,  
492 and aggregation of the climate data over archaeological periods (each of approximately four  
493 centuries here) may efface important variability. However, this evidence of broad consistency  
494 in climatic conditions and niches exploited suggests that climate was not a strong driver of  
495 settlement pattern in the study area during this period (and moreover the apparent sudden  
496 increase in site density in the Late Iron Age is in fact an artifact of time-averaging and was  
497 rather the result of gradual growth (cf. Isoardi, 2010)). Such (preliminary) negative evidence  
498 only becomes possible with downscaled data; with only coarse-grained data like that in Figure  
499 7a, questions like these, vital to considering potential impacts of past climate changes, cannot  
500 even be asked.

501

## 502 **5. Conclusions**

503

504 The simulated data produced by spatial and temporal downscaling capture both spatial  
505 variability and interannual variation in climatic factors, parameters fundamental to assessing  
506 the human consequences of climate changes. Examining such consequences at high  
507 resolution is necessary to analysis of the significance of climatic factors for such fundamental  
508 human activities as agriculture, and thus vital to the articulation of mechanisms linking  
509 climate and cultural change. There are drawbacks: downscaling adds a further layer of  
510 analysis, and can create a seductive precision when in fact it produces non-unique solutions  
511 that should be understood as reasonable but not necessarily accurate. However, *not*  
512 downscaling is also dangerous: it represents an *implicit* downscaling, in which coarse-grained  
513 data are presumed to indicate homogeneity within each granule, and understood as relevant at  
514 scales finer than those measured but without explicit mechanisms to relate regional to local or  
515 time-averaged to temporally-variable.

516 The methodology that we have presented here is straightforward to apply for any  
517 portion of the Holocene anywhere in the Mediterranean Basin using the same datasets, and  
518 the approach is adaptable to other regions and input data. The value of such data  
519 manipulation is analogous to what Lake (2015, p. 9) describes with reference to  
520 archaeological simulation modeling: it enables the virtual disaggregation of spatially and  
521 temporally coarse-grained data, and thus constitutes an important tool in shifting to a human  
522 scale of analysis. It can provide the raw material for further modeling and analysis focused  
523 on socioecological systems (advocated as a unique and significant contribution of  
524 archaeology to studies of sustainability and resilience; cf. Barton et al., 2012; Kohler and van  
525 der Leeuw, 2007; Van der Leeuw et al., 2011). Such modeling often requires higher-  
526 resolution and larger-scale data than that generally available from paleoclimate archives;  
527 indeed one of the benefits of such models is that they mandate explicit consideration of data  
528 requirements. The problem is not uniquely archaeological: developing agent-based models,  
529 agroecosystem models, or erosion models at scales directly relatable to human experience and  
530 decision-making is as much a challenge for socioecological science of the present as of the  
531 past. Downscaling tools are thus as needed in present-day modeling as in archaeological

532 simulation, and are vital for considering, for instance, the specific implications at local scales  
533 – i.e., the human impacts – of the 1.5 - 2 °C of global warming targeted by the COP21  
534 agreement. Methodologies like that presented here thus add needed components to the  
535 analytical toolkit for past human-environment dynamics, and potentially contribute to  
536 exploration of present and future human-environment dynamics as well.

---

537

538

### 539 **List of Figures**

540 **Figure 1:** Area of the case study.

541 **Figure 2:** Annual means (calculated from monthly values) of Holocene temperature (ADT)  
542 and precipitation (TMP) for the study area in centennial steps, from the HolCR dataset (Guiot  
543 and Kaniewski 2015) adjusted by using CNRM2014 data as a modern reference. Data on %  
544 cloudiness is also included, but not plotted here.

545 **Figure 3:** Mean values (ADT and TMP) of each of the 24 CNRM2014 datapoints within the  
546 study area for all points within the study area for the period 1950-2005 – i.e., the spatial  
547 variability in temperature and precipitation over a 56-year span. Labels denote the range of  
548 variability for each month.

549 **Figure 4:** Diachronic variability in ADT and TMP in the HolCR dataset for the cell including  
550 the study area, throughout the Holocene (data centered but not scaled).

551 **Figure 5:** Spatially downscaled monthly rasters for 2400 BP, the coolest period of the  
552 Holocene, with 100m contours derived from the SRTM30 DEM.

553 **Figure 6:** Temporally downscaled annual means of temperature (ADT) and precipitation  
554 (TMP) for the period 4200-4000 BP in the study area, with HolCR datapoints (solid circles)  
555 for reference. Inter-annual variability is based on the range and standard deviation of modern  
556 (CNRM2014) data, and the means and trends of the time series provided by the HolCR values  
557 (see Section 3.2.2).

558 **Figure 7: a)** Example of HolCR data for October 4000 BP, with CNRM2014 datapoints  
559 (black circles) and 100m elevation contours derived from the SRTM30 DEM. The source  
560 data provides monthly values like this in centennial steps. **b)** After spatial downscaling,  
561 values for March 4000 BP (middle panel) are spatially variable, and can be temporally  
562 downscaled for intervening years following centennial trends and modern interannual  
563 variability (e.g., illustrated in the nine panels here, the month of March for 4004 BP - 3096  
564 BP).

565 **Figure 8:** Early (green diamonds) and newly established Late (red triangles) Iron Age  
566 occupation and agricultural sites, plotted on 300m raster of mean annual TMP and standard  
567 deviation in TMP for the Early Iron Age and Late Iron Age (approximately 2700-2400 and  
568 2400-2002 BP, respectively). Boxplots indicate precipitation niches occupied by occupation  
569 and agricultural sites in the Early and Late Iron Age: each datapoint represents the mean TMP  
570 over the period within a 200m buffer around a site.

571

### 572 **List of Tables**

573 **Table 1:** Geographic variables and their predictive utility in the spatial downscaling process.

574 **Table 2:** Data sources.

575 **Table 3:** Monthly temperatures from HolCR and downscaling results for the study area at  
576 2400 BP.

577

### 578 **Acknowledgements**

579 Research has been funded by Labex OT-Med (ANR-11-LABEX-0061), the AMEDEES  
580 project, supported by A\*MIDEX project 11-IDEX-0001-02, “Investissements d’Avenir”

581 French Government project of the French National Research Agency (ANR) and by  
582 ECCOREV (AMEDEES-DB project). We thank the other members of the AMENOPHYS  
583 and AMEDEES projects, particularly Alberte Bondeau, Loup Bernard, Eneko Hiriart, Nobu  
584 Hanaki, and Sylvie Thoron. The paper has been considerably improved thanks to the  
585 thoughtful and constructive comments of two anonymous reviewers. The archaeological data  
586 in Figure 8, from the Patriarche database  
587 ([http://www.culturecommunication.gouv.fr/Politiques-ministerielles/Archeologie/Etude-  
589 recherche/Carte-archeologique-nationale](http://www.culturecommunication.gouv.fr/Politiques-ministerielles/Archeologie/Etude-<br/>588 recherche/Carte-archeologique-nationale)), were kindly provided by the Ministère de la  
Culture et de la Communication (DRAC PACA/SRA).

---

590  
591  
592  
593  
594

### **References cited**

- 595 Barton, C.M., Ullah, I., Bergin, S.M., Mitasova, H., Sarjoughian, H., 2012. Looking for the  
596 future in the past: Long-term change in socioecological systems. *Ecological Modelling*  
597 241, 42–53.
- 598 Barton, C.M., Ullah, I.I., Bergin, S., 2010. Land use, water and Mediterranean landscapes:  
599 modelling long-term dynamics of complex socio-ecological systems. *Philosophical*  
600 *Transactions of the Royal Society A: Mathematical, Physical and Engineering Sciences*  
601 368, 5275–5297. <https://doi.org/10.1098/rsta.2010.0193>
- 602 Berger, J.-F., Guilaine, J., 2009. The 8200 cal BP abrupt environmental change and the  
603 Neolithic transition: A Mediterranean perspective. *Quaternary International* 200, 31–49.
- 604 Bierkens, M., Finke, P., De Willigen, P., 2000. Upscaling and downscaling methods for  
605 environmental research. Kluwer Academic, Dordrecht.
- 606 Bivand, R., Yu, D., 2015. *spgwr: Geographically Weighted Regression*.
- 607 Bivand, R.S., 2015. Geographically Weighted Regression [WWW Document]. URL  
608 <https://cran.r-project.org/web/packages/spgwr/vignettes/GWR.pdf>
- 609 Blondel, J., Aronson, J., Bodiou, J.Y., Boeuf, G., 2010. *The Mediterranean region: biological*  
610 *diversity in space and time*, 2nd ed. Oxford University Press, Oxford.
- 611 Bocinsky, R.K., Kohler, T.A., 2014. A 2,000-year reconstruction of the rain-fed maize  
612 agricultural niche in the US Southwest. *Nature Communications* 5, 5618.
- 613 Box, G.E., 1979. Robustness in the strategy of scientific model building, in: Launer, R.L.,  
614 Wilkinson, G.N. (Eds.), *Robustness in Statistics*. Academic Press, New York, pp. 201–236.
- 615 Braje, T.J., 2015. Earth systems, human agency, and the Anthropocene: Planet Earth in  
616 the human age. *Journal of Archaeological Research* 23, 369–396.
- 617 Brayshaw, D.J., Rambeau, C.M., Smith, S.J., 2011. Changes in Mediterranean climate  
618 during the Holocene: Insights from global and regional climate modelling. *The Holocene*  
619 21, 15–31.
- 620 Büntgen, U., Tegel, W., Nicolussi, K., McCormick, M., Frank, D., Trouet, V., Kaplan, J.O.,  
621 Herzig, F., Heussner, K.U., Wanner, H., Luterbacher, J., Esper, J., 2011. 2500 Years of  
622 European Climate Variability and Human Susceptibility. *Science* 331, 578–582.
- 623 Burke, A., Levavasseur, G., James, P.M.A., Guiducci, D., Izquierdo, M.A., Bourgeon, L.,  
624 Kageyama, M., Ramstein, G., Vrac, M., 2014. Exploring the impact of climate variability  
625 during the Last Glacial Maximum on the pattern of human occupation of Iberia. *Journal*

626 of Human Evolution 73, 35–46.

627 Carozza, L., Berger, J.-F., Burens, A., Marcigny, C., 2015. Society and environment in  
628 Southern France from the 3rd millennium BC to the beginning of the 2nd millennium BC:  
629 2200 BC a tipping point? *Tagungen des Landesmuseums für Vorgeschichte Halle* 12,  
630 333–362.

631 Contreras, D.A., 2017. Correlation is Not Enough – Building Better Arguments in the  
632 Archaeology of Human-Environment Interactions, in: Contreras, D.A. (Ed.), *The*  
633 *Archaeology of Human-Environment Interaction: Strategies for Investigating*  
634 *Anthropogenic Landscapes, Dynamic Environments, and Climate Change in the Human*  
635 *Past*. Routledge, New York, pp. 3–22.

636 Contreras, D.A., Bondeau, A., Guiot, J., Kirman, A., Hiriart, E., Bernard, L., Suarez, R., Fader,  
637 M., in press. From Paleoclimate Variables to Prehistoric Agriculture: Using a Process-  
638 Based Agroecosystem Model to Simulate the Impacts of Holocene Climate Change on  
639 Potential Prehistoric Agricultural Productivity in Provence, France. *Quaternary*  
640 *International*.

641 Crutzen, P.J., Steffen, W., 2003. How long have we been in the Anthropocene era?  
642 *Climatic Change* 61, 251–257.

643 Currie, T.E., Bogaard, A., Cesaretti, R., Edwards, N., Francois, P., Holden, P., Hoyer, D.,  
644 Korotayev, A., Manning, J., Moreno Garcia, J.C., Oyebamiji, O.K., Petrie, C., Turchin, P.,  
645 Whitehouse, H., Williams, A., 2015. Agricultural productivity in past societies: Toward an  
646 empirically informed model for testing cultural evolutionary hypotheses. *Climodynamics*  
647 6, 24–56.

648 d’Alpoim Guedes, J., Manning, S., Bocinsky, R.K., 2016. A 5,500-Year Model of Changing  
649 Crop Niches on the Tibetan Plateau. *Current Anthropology* 57, 1–6.

650 Erickson, C.L., 2000. The Lake Titicaca Basin: A Precolumbian Built Landscape, in: Lentz,  
651 D.L. (Ed.), *Imperfect Balance: Landscape Transformations in the Precolumbian*  
652 *Americas*. Cambridge University Press, New York, pp. 311–356.

653 Erlandson, J.M., Braje, T.J., 2013. Archeology and the Anthropocene. *Anthropocene* 4, 1–  
654 7.

655 Finné, M., Holmgren, K., Sundqvist, H.S., Weiberg, E., Lindblom, M., 2011. Climate in the  
656 eastern Mediterranean, and adjacent regions, during the past 6000 years - A review.  
657 *Journal of Archaeological Science* 38, 3153–3173.

658 Forkel, M., Carvalhais, N., Verbesselt, J., Mahecha, M.D., Neigh, C.S., Reichstein, M., 2013.  
659 Trend change detection in NDVI time series: Effects of inter-annual variability and  
660 methodology. *Remote Sensing* 5, 2113–2144.

661 Forkel, M., Wutzler, T., 2015. greenbrown - land surface phenology and trend analysis. A  
662 package for the R software.

663 Fowler, H.J., Blenkinsop, S., Tebaldi, C., 2007. Linking climate change modelling to  
664 impacts studies: recent advances in downscaling techniques for hydrological modelling.  
665 *International Journal of Climatology* 27, 1547–1578.

666 Gauthier, N., 2016. The spatial pattern of climate change during the spread of farming  
667 into the Aegean. *Journal of Archaeological Science* 75, 1–9.

668 Gorenflo, L., Gale, N., 1986. Population and productivity in the Teotihuacan Valley:  
669 changing patterns of spatial association in prehispanic central Mexico. *Journal of*  
670 *Anthropological Archaeology* 5, 199–228.

671 GRASS Development Team, 2016. Geographic Resources Analysis Support System  
672 (GRASS GIS) Software, Version 7.0. Open Source Geospatial Foundation.

673 Guiot, J., Kaniewski, D., 2015. The Mediterranean Basin and Southern Europe in a  
674 warmer world: what can we learn from the past? *Frontiers in Earth Science* 3, 1–16.

675 Harris, I., Jones, P., Osborn, T., Lister, D., 2014. Updated high-resolution grids of monthly  
676 climatic observations—the CRU TS3.10 Dataset. *International Journal of Climatology* 34,  
677 623–642.

678 Hastie, T.J., Tibshirani, R.J., 1990. *Generalized Additive Models*. Chapman and Hall/CRC,  
679 London.

680 Hijmans, R.J., van Etten, J., 2016. *raster: Geographic data analysis and modeling*.

681 Isoardi, D., 2010. Archéodémographie des sociétés protohistoriques de Sud-Est de la  
682 France. *Arqueología Espacial* 28, 265–284.

683 Joly, D., Brossard, T., Cardot, H., Cavailles, J., Hilal, M., Wavresky, P., 2010. Temperature  
684 interpolation based on local information: the example of France. *International Journal of*  
685 *Climatology* 31, 2141–2153.

686 Kaniewski, D., Guiot, J., Van Campo, E., 2015. Drought and societal collapse 3200 years  
687 ago in the Eastern Mediterranean: a review. *Wiley Interdisciplinary Reviews: Climate*  
688 *Change* 6, 369–382.

689 Kaplan, J.O., Krumhardt, K.M., Ellis, E.C., Ruddiman, W.F., Lemmen, C., Klein Goldewijk, K.,  
690 2010. Holocene carbon emissions as a result of anthropogenic land cover change. *The*  
691 *Holocene*. <https://doi.org/10.1177/0959683610386983>

692 Kintigh, K.W., Altschul, J.H., Beaudry, M.C., Drennan, R.D., Kinzig, A.P., Kohler, T.A., Limp,  
693 W.F., Maschner, H.D.G., Michener, W.K., Pauketat, T.R., Peregrine, P., Sabloff, J.A.,  
694 Wilkinson, T.J., Wright, H.T., Zeder, M.A., 2014. Grand challenges for archaeology.  
695 *Proceedings of the National Academy of Sciences* 111, 879–880.

696 Kintigh, K.W., Ingram, S.E., 2018. Was the drought really responsible? Assessing  
697 statistical relationships between climate extremes and cultural transitions. *Journal of*  
698 *Archaeological Science* 89, 25–31.

699 Kohler, T.A., Bocinsky, R.K., Cockburn, D., Crabtree, S.A., Varien, M.D., Kolm, K.E., Smith,  
700 S., Ortman, S.G., Kobti, Z., 2012. Modelling prehispanic Pueblo societies in their  
701 ecosystems. *Ecological Modelling* 241, 30–41.

702 Kohler, T.A., van der Leeuw, S.E., 2007. *The Model-based Archaeology of Socionatural*  
703 *Systems*. School for American Research Press, Santa Fe.

704 Kootker, L.M., van Lanen, R.J., Kars, H., Davies, G.R., 2016. Strontium isoscapes in The  
705 Netherlands. Spatial variations in 87 Sr/86 Sr as a proxy for palaeomobility. *Journal of*  
706 *Archaeological Science: Reports* 6, 1–13.

707 Korhonen, N., Venäläinen, A., Seppä, H., Järvinen, H., 2014. Statistical downscaling of a  
708 climate simulation of the last glacial cycle: temperature and precipitation over Northern  
709 Europe. *Climate of the Past* 10, 1489–1500.

710 Lake, M.W., 2015. Explaining the Past with ABM: On Modelling Philosophy, in: Wurzer,  
711 G., Kowarik, K., Reschreiter, H. (Eds.), *Agent-Based Modeling and Simulation in*  
712 *Archaeology*. Springer, Heidelberg, pp. 3–36.

713 Levavasseur, G., Vrac, M., Roche, D., Paillard, D., Guiot, J., 2013. An objective methodology  
714 for potential vegetation reconstruction constrained by climate. *Global and Planetary*  
715 *Change* 104, 7–22.



716 Levavasseur, G., Vrac, M., Roche, D., Paillard, D., Martin, A., Vandenberghe, J., 2011.  
717 Present and LGM permafrost from climate simulations: contribution of statistical  
718 downscaling. *Climate of the Past* 7, 1225–1246.

719 Lock, G., Molyneaux, B.L., 2006. *Confronting Scale in Archaeology: Issues of Theory and*  
720 *Practice*. Springer, New York.

721 Luterbacher, J., Xoplaki, E., Casty, C., Wanner, H., Pauling, A., Küttel, M., Brönnimann, S.,  
722 Fischer, E., Fleitmann, D., Gonzalez-Rouco, F.J., others, 2006. Mediterranean climate  
723 variability over the last centuries: a review. *Developments in Earth and environmental*  
724 *Sciences* 4, 27–148.

725 Mamani Pati, F., Clay, D.E., Smeltekop, H., 2011. Geospatial Management of Andean  
726 Technology by the Inca Empire, in: Clay, D.E., Shanahan, J.F. (Eds.), *GIS Applications in*  
727 *Agriculture, Volume Two: Nutrient Management for Energy Efficiency*. CRC Press, Boca  
728 Raton, pp. 255–264.

729 Martin, N., Carrega, P., Adnes, C., 2013. Downscaling À Fine Résolution Spatiale des  
730 Températures Actuelles et Futures par Modélisation Statistique des Sorties Aladin-  
731 Climat sur les Alpes-Maritimes (France). *Climatologie* 10, 51–74.

732 Morrison, K.D., 2015. Provincializing the Anthropocene. *Seminar* 673, 75–80.

733 NASA JPL, 2013. NASA Shuttle Radar Topography Mission Global 1 arc second number.

734 New, M., Lister, D., Hulme, M., 2002. A high-resolution data set of surface climate over  
735 global land areas. *Climate Research* 21, 1–25.

736 R Core Team, 2016. *R: A Language and Environment for Statistical Computing*. R  
737 Foundation for Statistical Computing, Vienna, Austria.

738 Robb, J., Pauketat, T.R., 2013. From moments to millennia: Theorizing scale and change  
739 in human history, in: Robb, J., Pauketat, T.R. (Eds.), *Big Histories, Human Lives: Tackling*  
740 *Problems of Scale in Archaeology*. School for Advanced Research Press, Santa Fe, NM, pp.  
741 3–33.

742 Roberts, N., Stevenson, T., Davis, B., Cheddadi, R., Brewster, S., Rosen, A., 2004. Holocene  
743 climate, environment and cultural change in the circum-Mediterranean region, in:  
744 Battarbee, R.W., Gasse, F., Stickley, C.E. (Eds.), *Past Climate Variability through Europe*  
745 *and Africa*. Springer, Dordrecht, pp. 343–362.

746 Robinson, S.A., Black, S., Sellwood, B.W., Valdes, P.J., 2006. A review of palaeoclimates  
747 and palaeoenvironments in the Levant and Eastern Mediterranean from 25,000 to 5000  
748 years BP: setting the environmental background for the evolution of human civilisation.  
749 *Quaternary Science Reviews* 25, 1517–1541.  
750 <https://doi.org/10.1016/j.quascirev.2006.02.006>

751 Ruddiman, W.F., 2013. The Anthropocene. *Annual Review of Earth and Planetary*  
752 *Sciences* 41, 45–68.

753 Schwindt, D.M., Bocinsky, R.K., Ortman, S.G., Glowacki, D.M., Varien, M.D., Kohler, T.A.,  
754 2016. The Social Consequences of Climate Change in the Central Mesa Verde Region.  
755 *American Antiquity* 81, 74–96.

756 Seltzer, G.O., Hastorf, C., 1990. Climatic Change and Its Effect on Prehispanic Agriculture  
757 in the Central Peruvian Andes. *Journal of Field Archaeology* 17, 397–414.

758 Smith, B.D., Zeder, M.A., 2013. The onset of the Anthropocene. *Anthropocene* 4, 8–13.

759 Smith, M.E., Feinman, G.M., Drennan, R.D., Earle, T., Morris, I., 2012. Archaeology as a  
760 social science. *Proceedings of the National Academy of Sciences* 109, 7617–7621.

- 761 Spiridonov, V., Déqué, M., Somot, S., 2005. ALADIN-CLIMATE: from the origins to present  
762 date. ALADIN Newsletter 29, 89–92.
- 763 Stein, J.K., 1993. Scale in archaeology, geosciences, and geoarchaeology. Geological  
764 Society of America Special Papers 283, 1–10.
- 765 Van der Leeuw, S., Costanza, R., Aulenbach, S., Brewer, S., Burek, M., Cornell, S., Crumley,  
766 C.L., Dearing, J.A., Downy, C., Graumlich, L.J., Heckbert, S., Hegmon, M., Hibbard, K.,  
767 Jackson, S.T., Kubiszewski, I., Sinclair, P., Sörlin, S., Steffen, W., 2011. Toward an  
768 integrated history to guide the future. *Ecology and Society* 16.
- 769 Van der Leeuw, S., Redman, C., 2002. Placing archaeology at the center of socio-natural  
770 studies. *American Antiquity* 67, 597–605.
- 771 Vidal, J.-P., Martin, E., Franchistéguy, L., Baillon, M., Soubeyroux, J.-M., 2010. A 50-year  
772 high-resolution atmospheric reanalysis over France with the Safran system.  
773 *International Journal of Climatology* 30, 1627–1644.
- 774 Vrac, M., Marbaix, P., Paillard, D., Naveau, P., 2007. Non-linear statistical downscaling of  
775 present and LGM precipitation and temperatures over Europe. *Climate of the Past* 3,  
776 669–682.
- 777 Weinelt, M., Schwab, C., Kneisel, J., Hinz, M., 2015. Climate and societal change in the  
778 western Mediterranean area around 4.2 ka BP, in: Meller, H., Arz, H.W., Jung, R., Risch, R.  
779 (Eds.), *2200 BC- A Climatic Breakdown as a Cause for the Collapse of the Old World?*  
780 *Landesmuseum für Vorgeschichte, Halle*, pp. 461–480.
- 781 Weninger, B., Clare, L., Rohling, E., Bar-Yosef, O., Böhner, U., Budja, M., Bundschuh, M.,  
782 Feurdean, A., Gebe, H.G., Jöris, O., Linstädter, J., Mayewski, P., Mühlenbruch, T.,  
783 Reingruber, A., Rollefson, G.O., Schyle, D., Thissen, L., Todorova, H., Zielhofer, C., 2009.  
784 *The Impact of Rapid Climate Change on Prehistoric Societies during the Holocene in the*  
785 *Eastern Mediterranean. Documenta Praehistorica* 36, 7–59.
- 786 Wiener, M., 2014. The Interaction of Climate Change and Agency in the Collapse of  
787 Civilizations ca. 2300–2000 BC. *Radiocarbon* 56, S1–S16.
- 788 Wilby, R.L., Charles, S.P., Zorita, E., Timbal, B., Whetton, P., Mearns, L.O., 2004. Guidelines  
789 for Use of Climate Scenarios Developed from Statistical Downscaling Methods  
790 (Supporting Material of the Intergovernmental Panel on Climate Change (IPCC)),  
791 Prepared on Behalf of Task Group on Data and Scenario Support for Impacts and Climate  
792 Analysis (TGICA). IPCC.
- 793 Willmes, M., Bataille, C.P., James, H.F., Moffat, I., McMorrow, L., Kinsley, L., Armstrong,  
794 R.A., Eggins, S., Grün, R., 2018. Mapping of bioavailable strontium isotope ratios in  
795 France for archaeological provenance studies. *Applied Geochemistry* 90, 75–86.
- 796 Wu, J., Li, H., 2006. Perspectives and Methods of Scaling, in: Wu, J., Jones, K.B., Li, H.,  
797 Loucks, O.L. (Eds.), *Scaling and Uncertainty Analysis in Ecology: Methods and*  
798 *Applications*. Springer, Dordrecht, pp. 14–42.
- 799 Zalasiewicz, J., Waters, C.N., Williams, M., Barnosky, A.D., Cearreta, A., Crutzen, P., Ellis, E.,  
800 Ellis, M.A., Fairchild, I.J., Grinevald, J., Haff, P.K., Hajdas, I., Leinfelder, R., McNeill, J.,  
801 Odada, E.O., Poirier, C., Richter, D., Steffen, W., Summerhayes, C., Syvitski, J.P.M., Vidas, D.,  
802 Wagreich, M., Wing, S.L., Wolfe, A.P., Zhisheng, A., Oreskes, N., 2015. When did the  
803 Anthropocene begin? A mid-twentieth century boundary level is stratigraphically  
804 optimal. *Quaternary International* 383, 196–203.

Table 1: Data sources.

Data source	Summary description	Variables used	Spatial resolution	Temporal resolution and span	Reference and data url
CNRM2014	Simulated dataset based on the limited-area aladin-Climate model (Aire Limited Adaptation Dynamic development InterNational) and corrected by a quantile-quantile method to SAFRAN (Vidal et al., 2010).	TAV, PAV	8km	Monthly values, 1950-2005	(Spiridonov et al., 2005); <a href="http://www.cnrm.meteo.fr/spip.php?article125">http://www.cnrm.meteo.fr/spip.php?article125</a> ; DRIAS Portal at <a href="http://www.drias-climat.fr/">http://www.drias-climat.fr/</a>
CRU	Global ridded climate dataset interpolated from 20 <sup>th</sup> -21 <sup>st</sup> century meteorological station data.	cld <sup>a</sup>	10 <sup>7</sup>	1951-2010	(Harris et al., 2014; New et al., 2002); <a href="https://crudata.uea.ac.uk/cru/data/hrg/tmc/">https://crudata.uea.ac.uk/cru/data/hrg/tmc/</a>
HolCR	Holocene climate reconstruction based on pollen data and an inverse vegetation model (BIOME4)	ADT, TMP, % cloudiness	2° latitude x 4° longitude	Monthly estimates in centennial steps; 10000 BP - present	(Guiot and Kaniewski, 2015); OT-Med data catalog at <a href="http://database.otmed.fr/geonetworkotmed/srv/eng/search -  54b9bf34-57ae-45ea-b455-9f90351e538f">http://database.otmed.fr/geonetworkotmed/srv/eng/search -  54b9bf34-57ae-45ea-b455-9f90351e538f</a>
SRTM30	digital elevation model	elevation <sup>b</sup>	30m	2000	(NASA JPL, 2013); <a href="http://dds.cr.usgs.gov/srtm/">http://dds.cr.usgs.gov/srtm/</a>

a. In fact the CRU dataset provides % sunniness, which must be subtracted from 100 to provide % cloudiness.

b. Although they were not ultimately used, we also tested elevation derivatives, e.g., slope, aspect, and irradiance.

Table 1: Data sources.

Data source	Summary description	Variables used	Spatial resolution	Temporal resolution and span	Reference and data url
CNRM2014	Simulated dataset based on the limited-area aladin-Climate model (Aire Limited Adaptation Dynamic development InterNational) and corrected by a quantile-quantile method to SAFRAN (Vidal et al., 2010).	TAV, PAV	8km	Monthly values, 1950-2005	(Spiridonov et al., 2005); <a href="http://www.cnrm.meteo.fr/spip.php?article125">http://www.cnrm.meteo.fr/spip.php?article125</a> ; DRIAS Portal at <a href="http://www.drias-climat.fr/">http://www.drias-climat.fr/</a>
CRU	Global gridded climate dataset interpolated from 20 <sup>th</sup> -21 <sup>st</sup> century meteorological station data.	cld <sup>a</sup>	10 <sup>7</sup>	1951-2010	(Harris et al., 2014; New et al., 2002); <a href="https://crudata.uea.ac.uk/cru/data/hrg/tmc/">https://crudata.uea.ac.uk/cru/data/hrg/tmc/</a>
HolCR	Holocene climate reconstruction based on pollen data and an inverse vegetation model (BIOME4)	ADT, TMP, % cloudiness	2° latitude x 4° longitude	Monthly estimates in centennial steps; 10000 BP - present	(Guiot and Kaniewski, 2015); OT-Med data catalog at <a href="http://database.otmed.fr/geonetworkotmed/srv/eng/search -  54b9bf34-57ae-45ea-b455-9f90351e538f">http://database.otmed.fr/geonetworkotmed/srv/eng/search -  54b9bf34-57ae-45ea-b455-9f90351e538f</a>
SRTM30	digital elevation model	elevation <sup>b</sup>	30m	2000	(NASA JPL, 2013); <a href="http://dds.cr.usgs.gov/srtm/">http://dds.cr.usgs.gov/srtm/</a>

a. In fact the CRU dataset provides % sunniness, which must be subtracted from 100 to provide % cloudiness.

b. Although they were not ultimately used, we also tested elevation derivatives, e.g., slope, aspect, and irradiance.

**Table 3: Monthly temperatures from HolCR and downscaling results for the study area at 2400 BP.**

	January	February	March	April	May	June	July	August	September	October	November	December
<b>HolCR value</b>	3.08	4.04	6.91	10.57	14.67	18.26	21.29	21.55	17.33	12.12	7.21	4.03
<b>spatial minimum</b>	-1.08	-0.35	1.33	5.04	9.00	12.69	15.75	16.35	12.36	7.40	2.88	0.05
<b>spatial maximum</b>	4.77	5.67	8.69	12.24	16.24	19.95	22.95	23.08	18.87	13.86	8.97	5.63

Figure 1  
[Click here to download high resolution image](#)



Figure 2  
[Click here to download high resolution image](#)

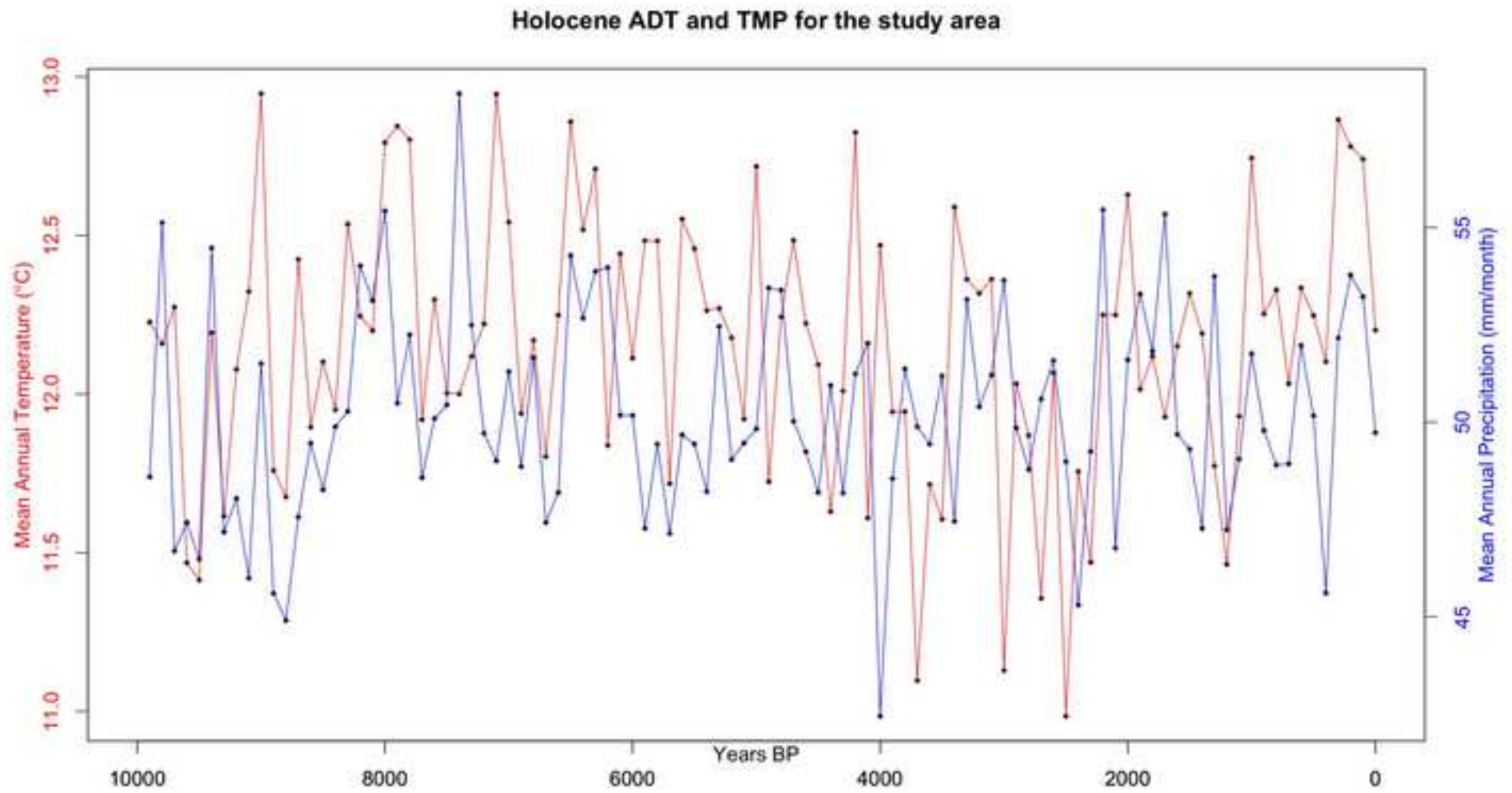


Figure 3  
[Click here to download high resolution image](#)

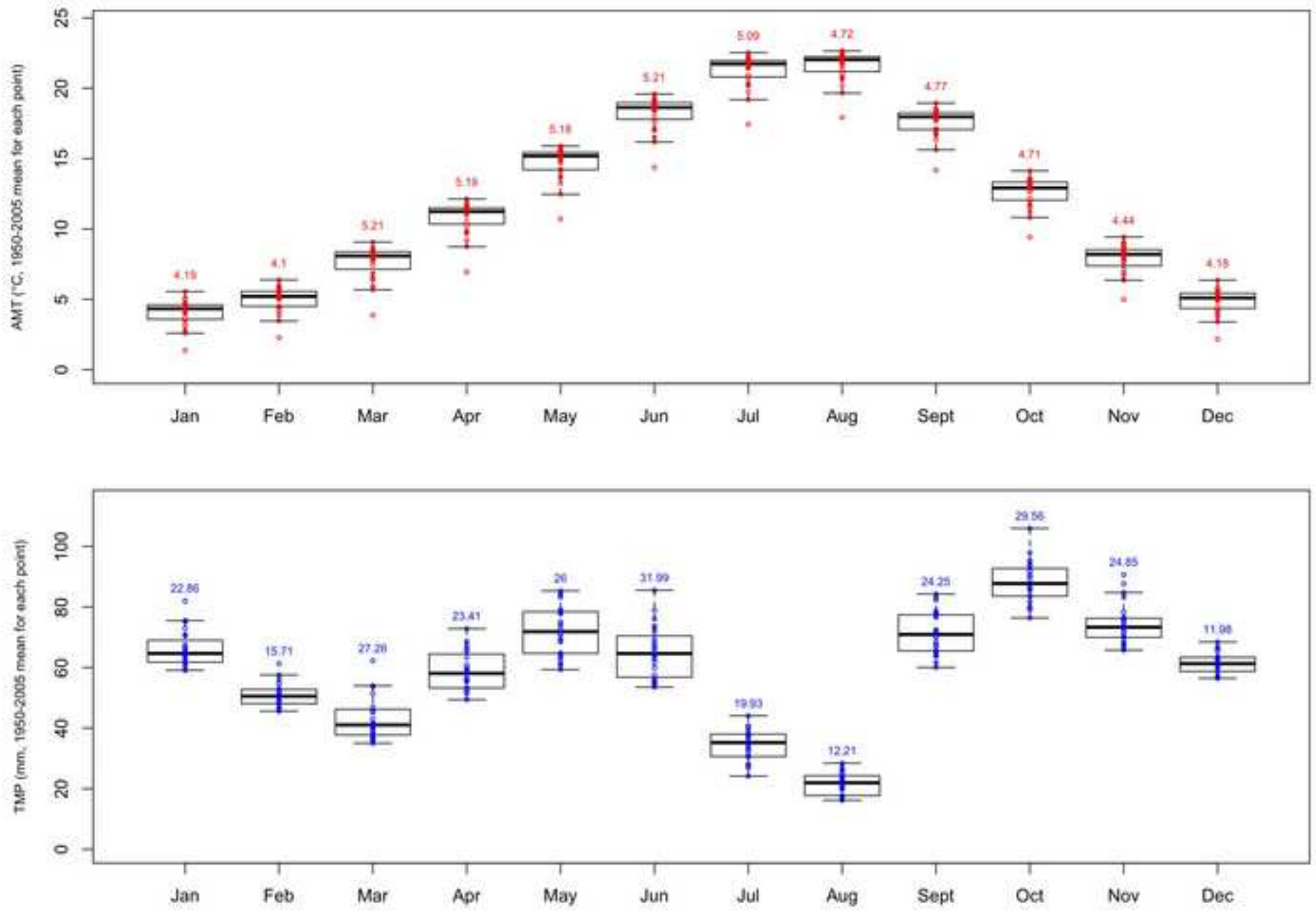




Figure 4  
[Click here to download high resolution image](#)

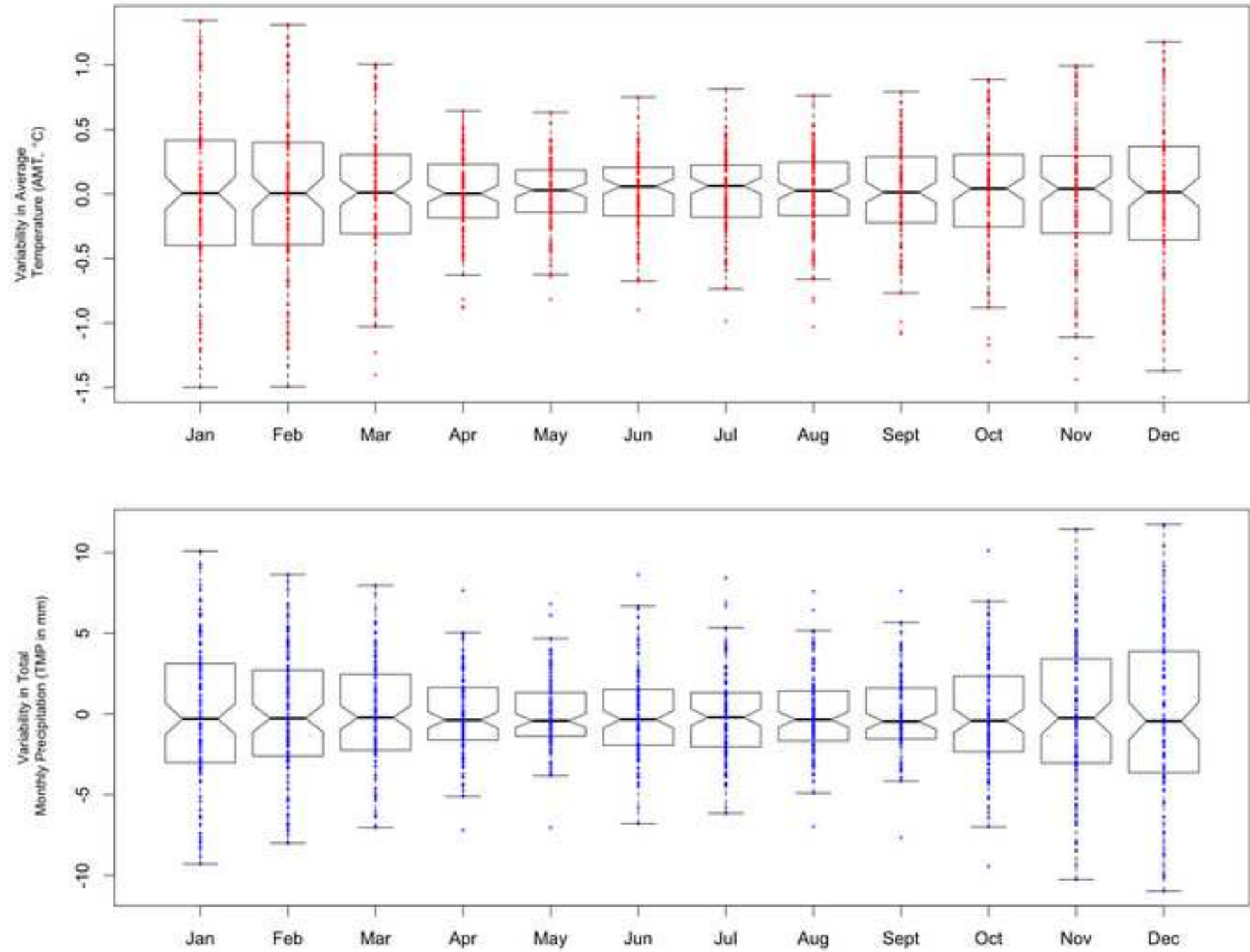
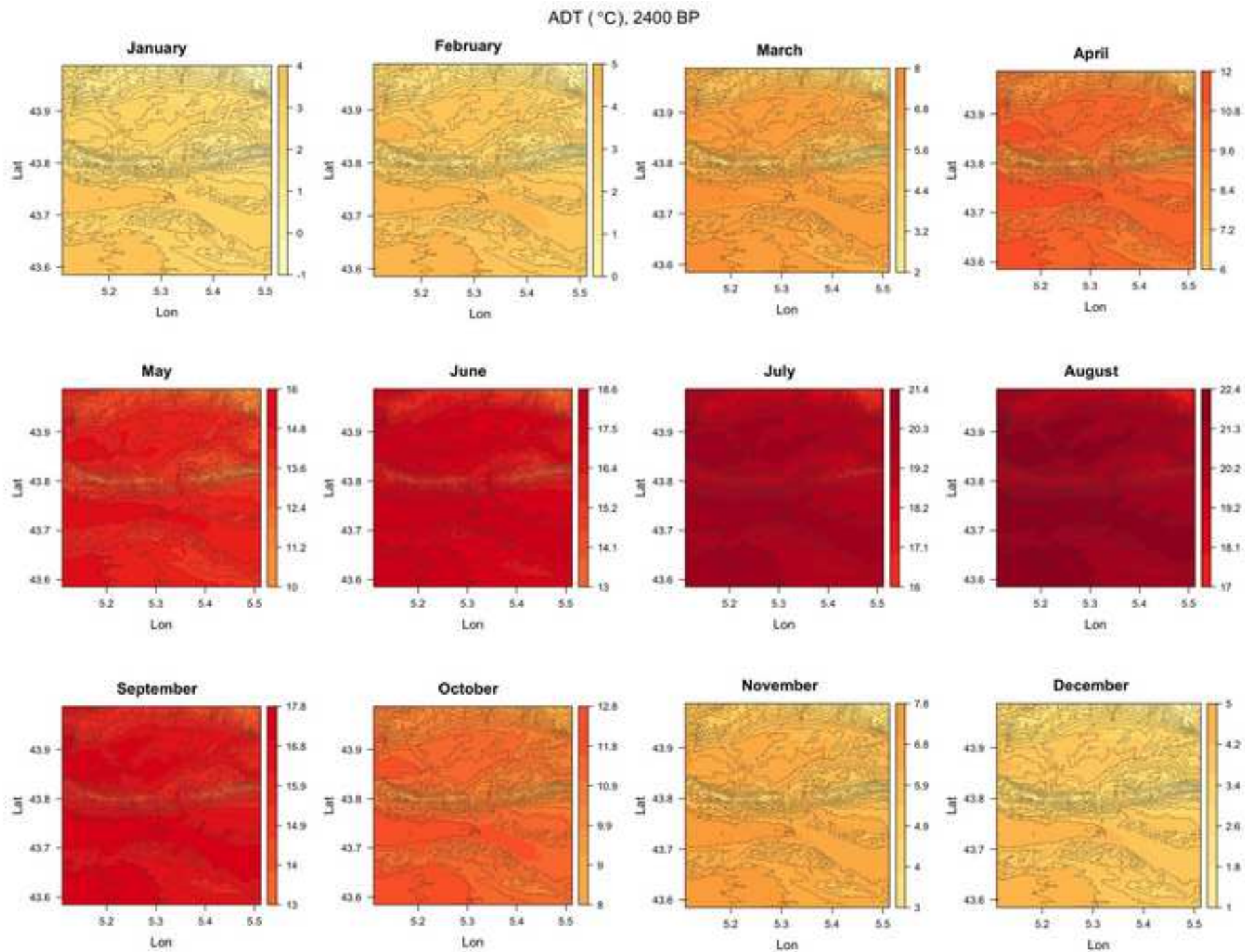
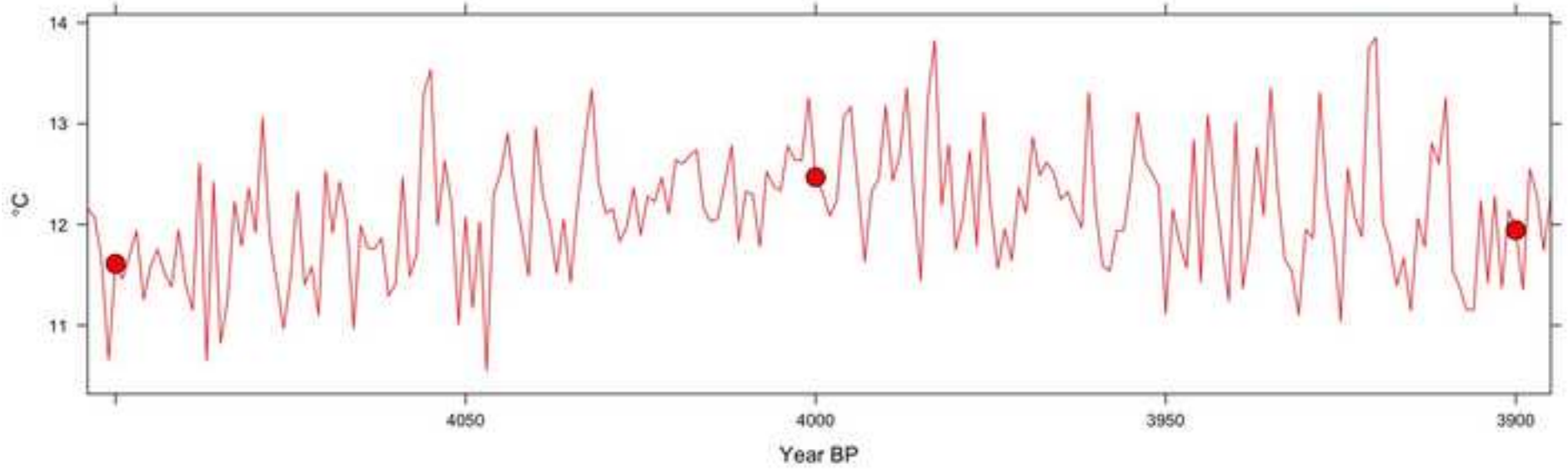


Figure 5  
[Click here to download high resolution image](#)



**Figure 6**  
[Click here to download high resolution image](#)

**Annual Temperature (Mean ADT)**



**Annual Precipitation (Mean TMP in mm)**

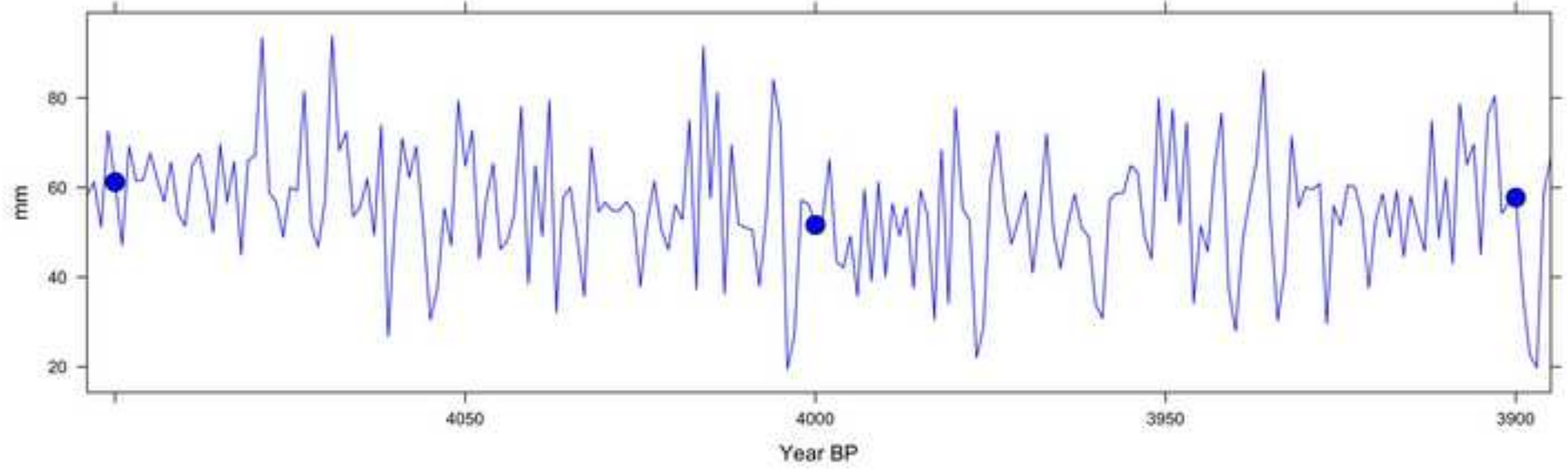
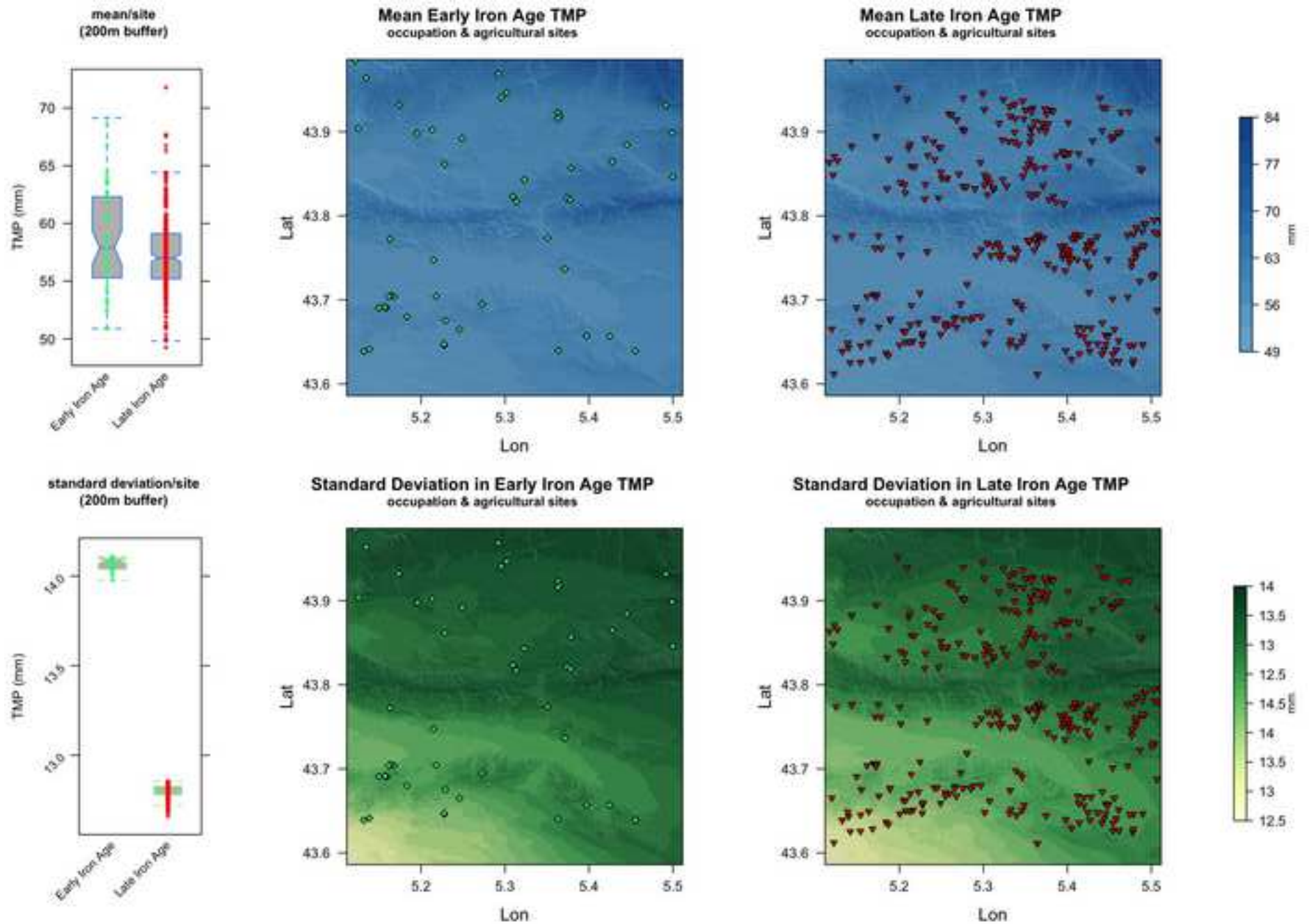




Figure 8

[Click here to download high resolution image](#)



**Supplementary Material - R code**

[Click here to download Supplementary Material: Rcode\\_forSI.r](#)